Desalination and Water Treatment
www.deswater.com

doi: 10.5004/dwt.2017.20239

70 (2017) 157–168
April

Thermal Na^+ conditioning of natural clinoptilolite for softening removal of aqueous Ca^{2+} from simulated cooling-water environment

S. Zhang[a,b,*], D. Wang[c], J.F. Zheng[a,b], Y.C. Chen[d], L.P. Sun[a,b]

[a] *School of Environmental and Municipal Engineering, Tianjin Chengjian University, Jinjing Road 26, Tianjin 300384, China, Tel. +86 13820306663; Fax: +86 022 23085000; email: zssci1203@163.com (S. Zhang), Tel. +86 13820081824; email: jianfen1605@163.com (J.F. Zheng), Tel. +86 13920097721; email: slpyqs@vip.sina.com (L.P. Sun)*
[b] *Tianjin Key Laboratory of Aquatic Science and Technology, Tianjin 300384, China*
[c] *Key Laboratory of Industrial Ecology and Environmental Engineering (MOE), School of Environmental Science and Technology, Dalian University of Technology, Linggong Road 2, Dalian 116024, China, Tel. +86 13940950507; email: wangdong@dlut.edu.cn*
[d] *McWong Environmental Engineering Co. Ltd., Shangcheng Road 1900, Shanghai 200135, China, Tel. +86 13816860769; email: 82670112@qq.com*

Received 21 April 2016; Accepted 29 September 2016

ABSTRACT

Na^+-conditioned clinoptilolite (NaCC) was evaluated as an efficient softener dealing with aqueous Ca^{2+} in cooling-water environments. Thermal Na^+ conditioning largely improved the softening capability of natural clinoptilolite, and the uptake of Ca^{2+} interestingly accelerated as solution temperature increased up to a level of 70°C (simulating spent cooling water). Batch study on fundamental parameters indicated that the adsorption kinetics and isotherms using NaCC could, respectively, be expressed by pseudo-first-order model and Langmuir equation. Ion exchange was determined as principal softening pathway being thermodynamically spontaneous and endothermic. In continuous column test, the breakthrough curves completed by NaCC can appreciably be delineated by Thomas and Yoon–Nelson models, demonstrating the viability on prediction of the equilibrium adsorbability and durability as significant operative parameters. Moderate pH level exhibited suitable enough for both the functionality and repeated use of NaCC. As a result of preliminary tests, Na^+ conditioning of clinoptilolite may be recommended as effective softening strategy serving for industrial cooling-water systems.

Keywords: Clinoptilolite; Cooling water; Softening; Fundamental parameter; Ion exchange

---

1. Introduction

Recirculating cooling-water system (RCWS) has drawn widespread application in petrochemistry, power, steel and metallurgy industries. The spent cooling water is produced in heat-exchange section of RCWS with dozens of degrees Celsius and needs to be conveyed into the cooling column (or tower) prior to recirculation for temperature-lowering purpose. Scaling problem frequently occurred [1–4] because in such hot-water environment, regular precipitant such as calcium carbonate readily forms alongside the wall of cooling equipment and covers the inside packing media. This adverse performance will ever pose severe failures on heat transfer and even partially clog channels within the packing zone against passage of water.

Scaling of industrial RCWS is typically originated from the residual bivalent hardness cations such as the calcium ion (i.e., Ca^{2+}) being representative in most cases. Addition of hydrosoluble inhibitor (e.g., ethylenediaminetetraacetic acid (EDTA) [5]) can alleviate the process of fouling, but hot-water environment induces considerable chemical decomposition and may in turn cause severe secondary contamination once overdosed. Chemical precipitation commonly allows an

---

[*] Corresponding author.

1944-3994/1944-3986 © 2017 Desalination Publications. All rights reserved.

effective softening, while for spent cooling water, solubility limitations of final product such as calcium carbonate make it rather difficult to realize relative abundant elimination of free Ca^{2+}, and moreover voluminous sludge will give rise to disposal problems. Adsorptive separation is thought to be a feasible resolution using functionalized material such as resins [6] and biomass adsorbents [7]. Concerning RCWS, however, resin particles have confining shortcomings as it swells in hot water leading to deformation or even rupture, and biomaterials suffer from lack of mechanical strength, inefficiency and limited reusability [8]. The need of scientific effort proceeds to develop functionalized adsorbent being effective and more suitable to work for RCWS in hydrothermal conditions.

Clinoptilolite can be exploited in a wide geographic distribution with aluminosilicate composition as the most abundant natural zeolite. It has tabular morphology with regular reticular structure containing easy-access cavities, and crystalline lattice distinguished by layers of tetrahedral formed by open channels of 8–10- membered rings [9]. Composing uniform pores and channels [10], numerous cavities of clinoptilolite are occupied by water molecules and exchangeable large ions such as Na^+, K^+ and Ca^{2+} species [11,12], enabling clinoptilolite to own the capability of removing small quantities of dissociative metal cations through a considerable pathway of ion exchange. Ion-exchange capacity of clinoptilolite is known to subject to the species (follow the selectivity sequence) and abundance of exchangeable cation attached on material surface, which relies on the procedures for surface modification concerning not only the surface chemistry of Si–O or Al–O tetrahedron structures but also the economy practicability. Thermal conditioning through boiling impregnation is easy-operative method to remove inert extra-framework cations, and in response locates more easily exchangeable cations in the framework channels of clinoptilolite. For example, pretreatment by NaCl-spiked matrix causes surface decoration of clinoptilolite with more active Na^+ sites [13]. Such way of chemical conditioning could therefore potentially ameliorate the adsorption capacity of natural clinoptilolite (NC) toward aqueous cations such as bivalent hardness ion. In addition to surface modifiability/recoverability, clinoptilolite has presented appreciable hydrothermal and mechanical stability owing largely to the crystalline structure. These merits are believed to be of practical significance for long-term utilization in RCWS of hydrothermal environment with temperature of tens of degree Celsius. Current reported researches using clinoptilolite as adsorbent cover treatment of cations including Ni^{2+} [14], Cu^{2+} [15], Zn^{2+} [16] and Mn^{2+} [17], but it is rarely reported the performance of clinoptilolite in case of hot-water environments such as for softening process. Therefore, it is incentive to further develop clinoptilolite with application potentiality for softening of cooling-water system.

In this work, thermal Na^+ conditioning of clinoptilolite was conducted as simplified pretreatment process, of which the functionalized product (i.e., NaCC) was investigated dealing with aqueous Ca^{2+} as typical hardness ion. The performances of NaCC were evaluated by batch and column experiments with increasing solution temperature up to 70°C (simulating the state of RCWS). Fundamental parameters were studied (in terms of adsorption isotherms, kinetics and thermodynamics); predictive models were employed aiming to achieve better process control; and effects of operative factors (such as solution pH, conditioning times and repeated utilization of NaCC) were investigated.

2. Materials and methods

2.1. Materials

Chemical reagents were all supplied by Kermel Reagent Co. Ltd. (Tianjin, China) and used as purchased in analytical purity, including calcium chloride ($CaCl_2$), sodium chloride (NaCl), hydrochloric acid (HCl) and sodium hydroxide (NaOH).

Clinoptilolite was exploited from Hulu Island of China and supplied by KangHua Science & Technology Co., Ltd. (Hulu-Island, China). Raw bulk material was broken to pieces, milled by mortar, screened to get small particles in diameters of 0.5–1 mm (14–35 mesh), boiled in distilled water to remove impurities and then dried overnight at 150°C. The obtained fine particles were regarded as natural clinoptilolite and labeled as "NC".

For pretreatment of Na^+-conditioning, 1 g NC sample was boiled in 50 mL NaCl solution (containing 15 wt% NaCl) for 30 min, washed by distilled water several times for surface cleaning and neutralization, and then dried at 150°C for about 24 h. The prepared solid sample was recorded as one-time thermal Na^+-conditioning, according to which *N*-time conditioning followed the same procedure.

2.2. Experiments

Schematic diagram for lab-scale experimental apparatus is illustrated in Fig. 1. Batch studies were performed in a series of glass reactors containing 50 mL $CaCl_2$ solution (with preset Ca^{2+} concentrations), and 1 g solid sample was added

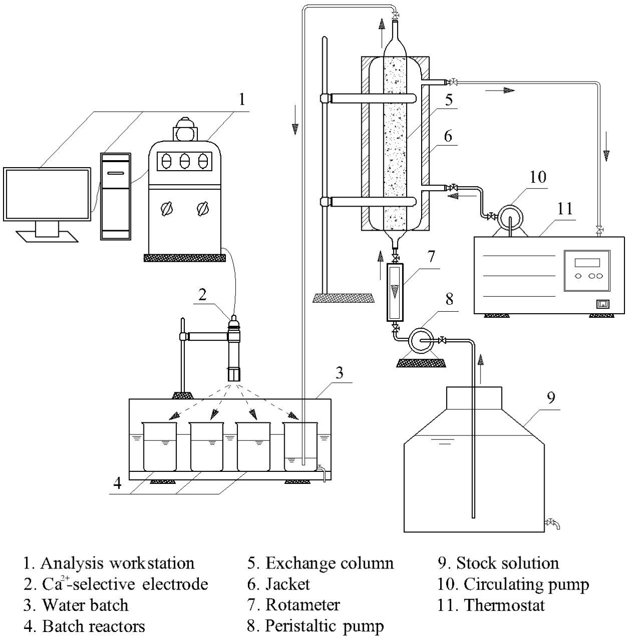

Fig. 1. The schematic diagram of lab-scale batch and minicolumn experiments.

for each test. Solution temperature was controlled by a water bath with an accuracy of ±0.02°C (TRW-327, IUCHI, Japan).

For continuous tests, a cylindrical minicolumn was packed with solid sample working in fixed-bed mode (internal diameter × column height = 10 mm × 200 mm). The amount of filling adsorbent was controlled at 11.5 g reaching a height very close to the top of reactor. The $CaCl_2$ stock solution was introduced at the bottom of reactor by peristaltic pump (inlet Ca^{2+} concentration of 400 mg/L), passed upward through the packing zone at flow rate of 3 mL/min, and then the effluent was collected from the top of reactor for further analysis (see Fig. 1). A thermal jacket containing circulating water was designed to control solution temperature in column using a thermostat with accuracy of ±0.5°C (Scientz Biotechnology Co., Ltd., China).

Unless otherwise specified, solution pH was not regulated for most experiments upon addition of NaCC (about 6.7 with 400 mg/L Ca^{2+}), because Na^+-conditioned clinoptilolite (NaCC) is much more selective toward Ca^{2+} than hydrogen ions (H^+) or its hydronium form (H_3O^+). All the reactions were completed under atmospheric pressure condition.

2.3. Analysis

Concentration of dissociative calcium ion was detected using Ca^{2+}-selective electrode supported by MIA-6 analytical workstation (Jiangsu, China). Solution pH was measured by digital pH meter (Cyber Scan pH1500).

For characterization of natural and NaCC: metal contents were evaluated by X-ray fluorescence apparatus (XRF-1800); X-ray diffraction (XRD) patterns were acquired using DX-3000 X-ray diffractometer (Shimadzu, Japan) with Cu Kα monochromatic radiations, operated at 40 kV and 100 mA; Fourier transform infrared (FT-IR) spectra were recorded between 400 and 4,000 cm^{-1} with Bruker Vector FT-IR spectrometer (sample amount was about 1 wt%; pure potassium bromide was utilized as reference); surface morphology was examined using scanning electron microscopy (SEM) (S4800, Hitachi, Japan); textural properties were determined by Autosorb-1 (Quantachrome, USA), for which adsorption/desorption isotherms of N_2 at about –196.15° were measured and the specific surface area (SSA) was calculated using the Brunauer–Emmett–Teller (BET) model.

3. Results and discussion

3.1. Material conditioning and characterization

Calcium cation commonly resides on the channels of NC in occupation of negative-charged sites, and thermal conditioning by active cations in exchange of localized calcium may enhance material affinity toward dissociative Ca^{2+} species. Fig. 2 shows the removal of free Ca^{2+} within an hour by clinoptilolites undergoing different times of Na^+-conditioning, for which the adsorption capability apparently enhanced as a function of replicated Na^+-conditioning. The frequent use of NaCl as a conditioning agent for further cation-exchange applications of zeolites is related to the crystal chemical features of Na cation, because sodium ions are the weakest bound ones and most easily exchanged with various cations from solutions [18,19]. It is clear that three-time Na^+ conditioning of clinoptilolite allowed an optimal adsorption rate of Ca^{2+} (up to 44% in 1 h, the corresponding material was labeled as NaCC). This is because the greater number of Na^+ sites per unit weight will accordingly allow higher exchange capacities, since negative surface charge of clinoptilolite was created once Al^{3+} replaces Si^{4+} in zeolitic structure was counterbalanced by Na cations [20].

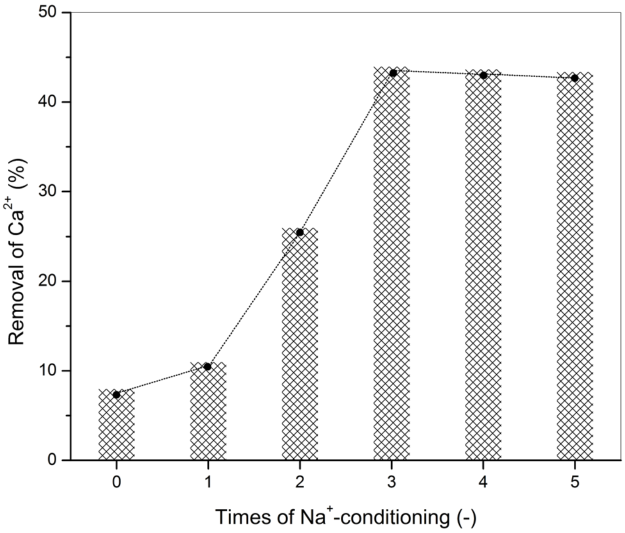

Fig. 2. Removal of aqueous Ca^{2+} by clinoptilolite undergoing different times of Na^+ conditioning (initial concentration of Ca^{2+} = 400 mg/L; temperature = 70°C; solution pH = 6.7; time = 1 h).

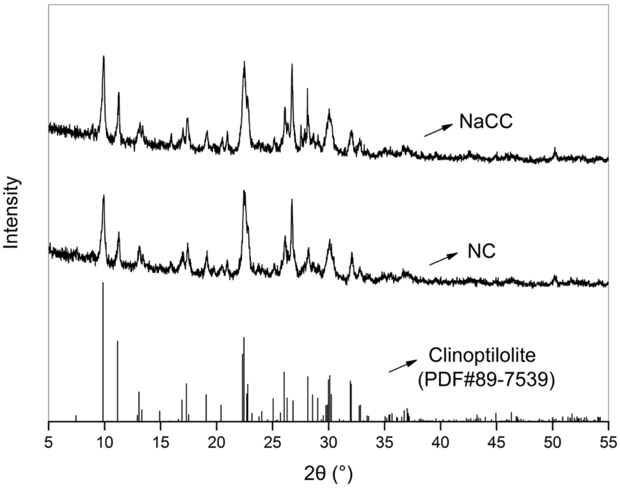

Fig. 3. XRD pattern of starting clinoptilolite (NC), three-time Na^+-conditioned clinoptilolite (NaCC) and clinoptilolite according to PDF-card.

Fig. 3 shows the XRD pattern of starting clinoptilolite (NC) and three-time NaCC. The employed NC presented in a well-crystallized structure, and according to PDF-card (#89-7539), it may be further classified as clinoptilolite type with simplified formula of $(Na_{0.52}K_{2.44}Ca_{1.48})(Al_{6.59}Si_{29.41}O_{72})(H_2O)_{28.64}$ (figure of merit is 1.7). For prepared NaCC sample, there is no sign on formation of halite (characteristic peaks of 35.819°

and 45.619°), which demonstrated that most sodium cations (Na^+) had successfully completed exchange and stabilized on extra-framework of NC.

Table 1 lists comparative characterization of NC and NaCC in terms of texture property and metal contents. The mass content of Na-element got elevated from 0.71% of starting material (i.e., NC) up to 3.82% of NaCC, while simultaneously the content of Ca-element clearly dropped from 3.64% of NC to 0.56% of NaCC. Noting there was no considerable change in amount of other metal elements coexisted, it can be inferred that most of Na^+ species has chemically replaced local calcium cations as a result of thermal ion exchange and attached on extra-framework of clinoptilolite. Accordingly, the exchange ability rapidly enhanced with 44.3% removal of Ca^{2+} by NaCC compared with that by NC with only no more than 8% (see Fig. 2). There were slight increases in SSA, pore volume and average pore size after thermal Na^+ conditioning (see Table 1), showing the chemical sweeping effect against some trace impurities on NC such as titanium (Ti), though relative amount of the major identified elements were not strictly conform to the standard formula of clinoptilolite. No additional removal of aqueous Ca^{2+} can be attained once Na^+ conditioning were conducted more than three times (see Fig. 2), implying a saturated Na^+ conditioning state and the dispensability for clinoptilolite to suffer a more frequent thermal pretreatment.

The surface morphology and framework structure of solid samples were examined by SEM images and FT-IR spectroscopy as illustrated in Fig. 4. Thermal pretreatment did not cause visible change of clinoptilolite surface morphology (Fig. 4(b)) compared with the starting material (Fig. 4(a)), and this phenomenon also mirrored the hydrothermal stability of clinoptilolite to work in cooling-water systems as can be indicated by XRD spectra. FT-IR results are shown in Fig. 4(c). The bands in the range of 450–1,200 cm^{-1} connected with the internal Si–O(Si) and Si–O(Al) vibrations in tetrahedra or alumino-/silico- oxygen bridges, among which the band of 600–800 cm^{-1} corresponds to pseudo-lattice vibrations of structural units (e.g., band of 710–760 cm^{-1} is due to the vibration of Al–O fragment) and at about 1,054 cm^{-1} characteristic band is assigned to the rings of SiO_4 and AlO_4 tetrahedra [21]. Bands in the range of 1,600–3,700 cm^{-1} are commonly related to the presence of OH^- groups and zeolitic water, as that observed at about 1,639 cm^{-1} lies in the deformation mode of absorbed water molecules and at about 3,625 cm^{-1} is connected with the vibrations of OH^- groups (on Si^{4+} or Al^{3+}) whose arrangement in the structure is systematic.

Generally, the aluminosilicate framework of NaCC presented quite similar to NC, indicating an intact molecular structure of material skeleton after frequent thermal treatment. Regarding the adsorption capability toward aqueous Ca^{2+}, three times of Na^+ conditioning should be more recommendable for pretreatment of NC, and performances of the prepared NaCC were systematically examined in the subsequent experiments.

3.2. Batch study

3.2.1. Kinetics

Adsorption kinetics can give a description on reaction rate along with time to reach the equilibrium, which should have a large dependence on the physical and chemical characteristics of adsorbent as well as the operating conditions (such as solution temperature). According to batch experiments, the evolutions of adsorbed Ca^{2+} amounts by NaCC over time were recorded under different temperatures. Results are shown in Fig. 5. A fast stage for uptake of Ca^{2+} by NaCC was exhibited within the first 6 h, which indicates a rapid initial transfer of free Ca cations from the liquid bulk into the near surface boundary layers of solid phase. This process was followed by a slower Ca^{2+} uptake that could be attributed to both the reduced driving force of liquid-to-solid mass transfer and diffusion from external sites to internal sites of NaCC. Eventually, the adsorbed Ca^{2+} amounts at about 25 h grew up to a level very close to equilibrium state (about 18.1 mg/g).

To examine the rate constant of Ca^{2+} adsorption, the Lagergren equation (i.e., first rate) and pseudo-second-order model were employed as demonstrated, respectively, by Eqs. (1) and (2):

$$\frac{dq_t}{dt} = k_1(q_e - q_t) \tag{1}$$

$$\frac{dq_t}{dt} = k_2(q_e - q_t)^2 \tag{2}$$

where q_t represents the adsorption amount of Ca^{2+} at time "t", mg/g; q_e represents the equilibrium adsorption amount of Ca^{2+}, mg/g; k_1 is the overall rate constant of pseudo-first-order model, min^{-1}; and k_2 is the overall rate constant of pseudo-second-order model, g/(mg·min).

Results of relevant parameters are listed in Table 2. The pseudo-first-order kinetic model with correlation coefficients (R^2) beyond 0.994 fits better with Ca^{2+} adsorption process compared with pseudo-second-order model ($R^2 < 0.984$), and the simulative results illustrated in Fig. 5 show more appreciable suitability of pseudo-first-order kinetic model. With

Table 1
Textural properties and chemical compositions of NC and NaCC

Type	SSA (m^2/g)	Pore		Major elements and contents (wt%)								
		Volume (cm^3/g)	Size (nm)									
NC	45.70	0.094	8.21	O	Si	Al	Ca	K	Fe	Na	Mg	Ti
				53.76	30.47	6.63	3.64	1.91	1.75	0.71	0.59	0.22
NaCC	48.17	0.101	8.40	O	Si	Al	Na	K	Fe	Ca	Mg	Cl
				51.24	33.13	6.36	3.82	1.95	1.57	0.56	0.46	0.38

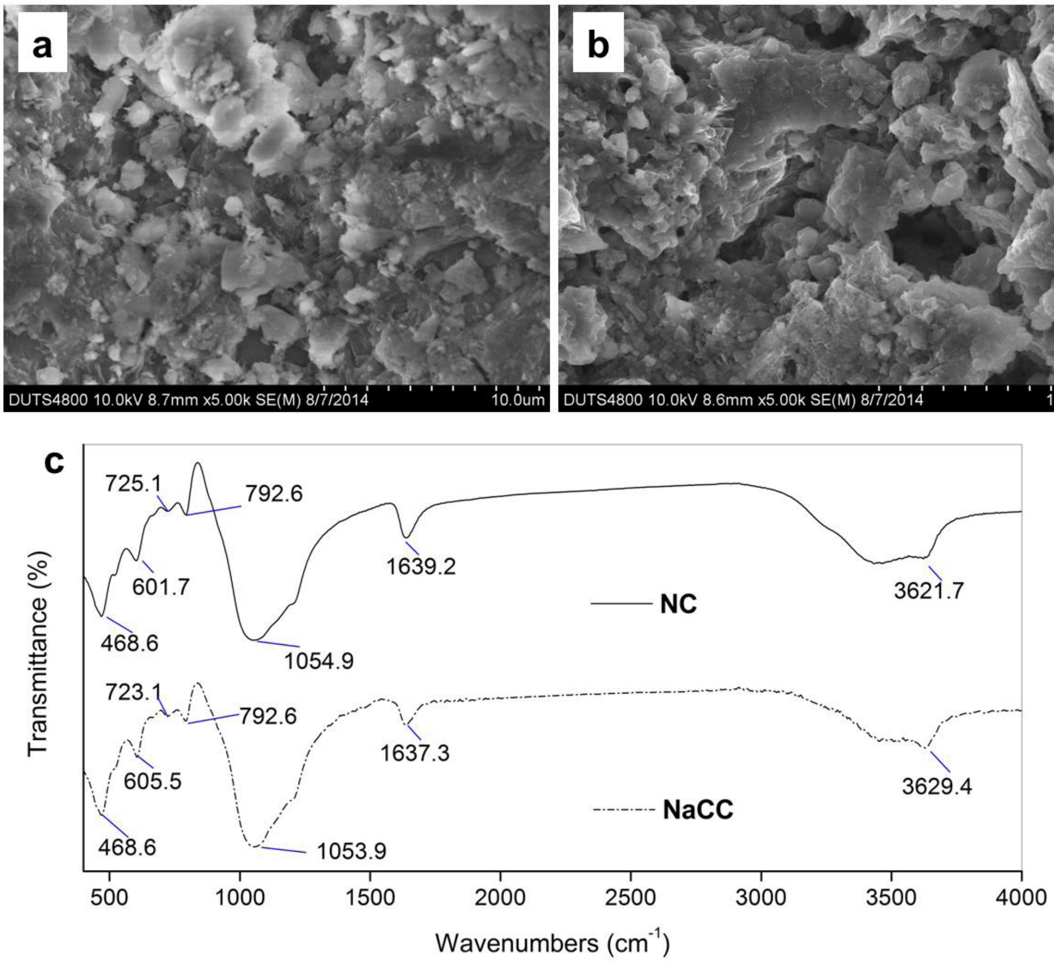

Fig. 4. SEM images of: (a) NC, (b) NaCC, and (c) FT-IR spectra of NC and NaCC.

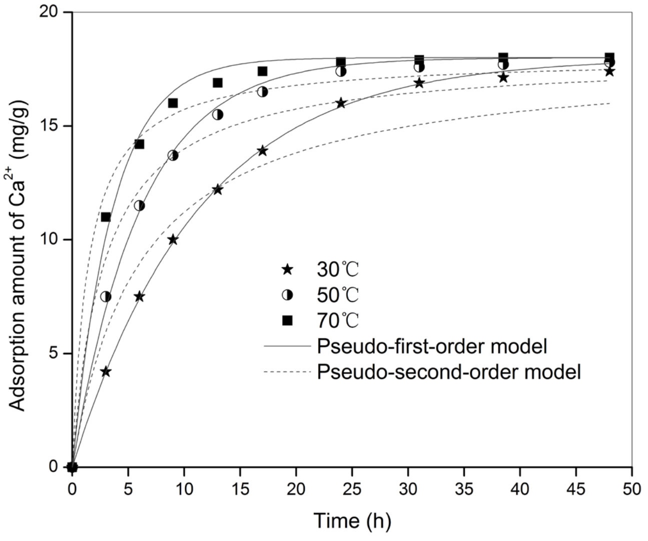

Fig. 5. Plot of adsorbed Ca^{2+} amount vs. time under respective solution temperature of 30°C, 50°C and 70°C (initial concentration of Ca^{2+} = 400 mg/L; solution pH = 6.7).

Table 2
Kinetic parameters for NaCC-induced adsorption of Ca^{2+} under different solution temperatures

Temperature (°C)	Pseudo-first-order		Pseudo-second-order	
	k_1 (min^{-1})	R^2	k_2 (g/(mg·min))	R^2
30	0.0884	0.999	0.00918	0.949
50	0.164	0.997	0.0194	0.968
70	0.277	0.994	0.0383	0.984

increasing solution temperature from 30°C to 70°C, the rate constant (i.e., k_1) sharply elevated from 0.0884 to 0.277 min^{-1} (see Table 4), which quantitatively demonstrates the positive impact of hydrothermal environment to accelerate the uptake of Ca^{2+} using NaCC. Accordingly, see Fig. 5, more rapid adsorption of Ca^{2+} took place under higher temperature of 70°C, and the equilibrium was reached ahead of time compared with scenarios under lower temperatures of 50°C and 30°C. The final adsorption amount of Ca^{2+} did not show clear distinction as temperature varied, since adsorption equilibrium was principally subject to the dynamic balance between bulk concentration of sorbate (i.e., Ca^{2+}) and that in solid–liquid interfacial region. Then residence time of adsorbent needs proper control regarding the fast-adsorption intervals in Fig. 5 to realize more efficient utilization of surface chemistry of NaCC.

3.2.2. Isotherms and thermodynamics

Sole application of kinetics model on adsorption on solid adsorbent may be oversimplified due to the process complexity containing property of adsorbent surfaces (homogeneity or heterogeneity) as well as the diversity of adsorption phenomena. Adsorption isotherm indicates how the target ions are partitioned between adsorbent and liquid phases at equilibrium state, and here, it is plotted by recording the amount of Ca^{2+} adsorbed as a function of initial concentrations in 50, 100, 200, 400, 600 and 800 mg/L for temperatures of 30°C, 50°C, and 70°C (see Fig. 6).

The Freundlich and Langmuir models were employed to evaluate the adsorption isotherm as, respectively, expressed in Eqs. (3) and (4):

$$q_e = k_f C_e^{\ n} \tag{3}$$

$$q_e = \frac{k_a q_m C_e}{1 + k_a C_e} \tag{4}$$

where q_e is the equilibrium amount of Ca^{2+} adsorbed per unit weight of adsorbent, mg/g; k_f and n are the Freundlich constants as respective indicators of adsorption capacity and reaction energy [22]; C_e is concentration of adsorbate at equilibrium state, mg/L; and k_a and q_m are the Langmuir constants, respectively, related to the adsorption equilibrium, L/mg, and the saturated monolayer adsorption capacity, mg/g.

The Langmuir isotherm assumes homogeneous surface for which adsorption free energy was independent on both the surface coverage and formation of sorbate-inhabited monolayer, while the Freundlich isotherm gives an assumption of surface heterogeneity and does not take into account the saturation of adsorption (the surface coverage being mathematically unlimited). Relevant parameters correlated to these two isotherm models were calculated as shown in Table 3. Experimental data generally correlated well with these two adsorption models, although q_m represents the monolayer adsorption capacity whereas k_f is considered to be the adsorption power [23]. The correlation coefficients (i.e., R^2) shows that the Langmuir model fits the results better than the Freundlich model, demonstrating the Langmuir type is more suitable to simulate the adsorption isotherms (refer to Fig. 6).

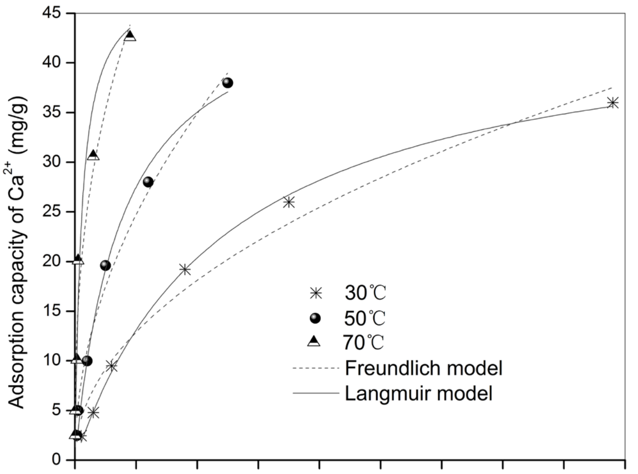

Fig. 6. Adsorption isotherms for various initial Ca^{2+} concentrations (solution pH = 6.7; sampling interval = 48 h).

The shape Langmuir isotherm was further investigated in terms of dimensionless constant separation factor (namely R_L) to determine the affinity between sorbate and sorbent. R_L can be calculated by Eq. (5) taking advantage of the parameter k_a determined in Langmuir model:

$$R_L = \frac{1}{1 + k_a C_0} \tag{5}$$

where C_0 represents the initial concentration of Ca^{2+}, mg/L.

R_L indicates four probabilities of adsorption isotherm as irreversible ($R_L = 0$), favorable ($0 < R_L < 1$), linear ($R_L = 1$) or unfavorable ($R_L > 1$) [24]. For different temperatures, the variations in separation factor with initial Ca^{2+} concentration are presented in Fig. 7. All the R_L values determined were in the range of 0–1 for this investigation, indicating that the adsorption of Ca^{2+} onto NaCC was favorable. Increment of initial Ca^{2+} concentration or elevation of solution temperature all resulted in reduction of R_L value, and 70°C exhibited to be particularly advantageous with most of R_L values approached zero. The remarkable enhancement of k_a from the Langmuir model with increasing temperature also infers that the adsorption of Ca^{2+} by clinoptilolite should be more vigorous in hot-water conditions.

Treatment of heavy metal ions from aqueous solution or wastewater by clinoptilolite was somewhere assumed to be accompanied by ion exchange and adsorption [25,26], while reaction process initiated by functionalized clinoptilolite for removal of Ca^{2+} as hardness ion was seldom reported. To this end, the energy of activation (E_a) for reaction was examined and can be formulated by linearized Arrhenius equation (Eq. (6)):

$$\ln k_1 = \ln A - \frac{E_a}{RT} \tag{6}$$

Table 3
Adsorption isotherms of Ca^{2+} by activated clinoptilolite under different temperature

Temperature (°C)	Langmuir			Freundlich		
	q_m (mg/g)	k_a (L/mg)	R^2	k_f	n	R^2
30	45.71	0.041	0.998	4.156	0.491	0.977
50	47.35	0.132	0.992	7.849	0.498	0.988
70	48.75	0.953	0.973	19.535	0.368	0.963

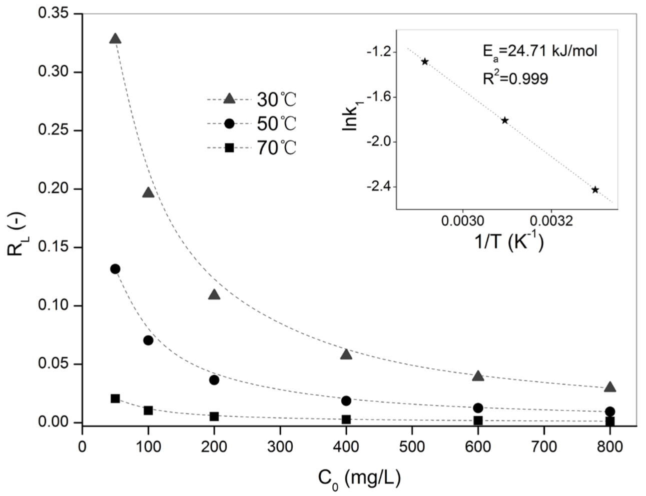

Fig. 7. Evolution of separation factor (R_L) vs. initial Ca^{2+} concentration (C_0) under respective solution temperature of 30°C, 50°C and 70°C.

where A represents the Arrhenius factor, min^{-1}; E_a is the activation energy, kJ/mol; R is the gas constant, 8.314×10^{-3} kJ/(mol·K); and T is the solution temperature, K.

The value of E_a (24.71 kJ/mol) was determined from the slope of k_1 vs. $1/T$ plots as shown by the inset of Fig. 7, which can give information that the adsorption process belongs to physical-sorption (normally had activation energy of 5–40 kJ/mol [27]). Regarding that chemical-sorption had much higher activation energy of 40–800 kJ/mol, it is assumed that there was no occurrence of considerable chemical behavior such as, if any, precipitation-induced aggregation of Ca^{2+} populations on HO groups of the Brǿnsted acid center. Moreover, the value of E_a presented not to be in the range accounting for kinetic adsorption with energies usually greater than 25–30 kJ/mol [28] (characterized by transferred or shared electrons), and thus, diffusion-controlled adsorption process may be assigned to this study occurring adjacent to solid–liquid interface (i.e., mass transfer limitations). Then it may be inferred that the performance of ion-exchange governs the uptake of dissociative Ca^{2+} by numerous Na^+-occupied sites formed in situ on surface region of clinoptilolite, and any other negatively charged sites contributed by aluminosilicate framework are not likely to make apparent contributions.

The Gibbs free energy (ΔG°) for each temperature can be determined by Eq. (7) using the obtained Langmuir constant (i.e., k_a), and the entropy (ΔS°) and enthalpy (ΔH°) were calculated from Van 't Hoff equation [29] (Eq. (8)):

$$\Delta G^\circ = -RT\ln(k_a \cdot 40 \cdot 10^3) \tag{7}$$

$$\Delta G^\circ = \Delta H^\circ - T\Delta S^\circ \tag{8}$$

Results of the thermodynamic parameters are listed in Table 4. The negative values for Gibbs free energy revealed that adsorption of Ca^{2+} by NaCC was spontaneous. Once solution temperature increased, the absolute value of ΔG° accordingly grew up, suggesting that the degree of exchange spontaneity got promoted in hot-water conditions. The outcome of ΔH° demonstrated the exchange process is generally endothermic, and positive value of ΔG° reflected the entropy-driven nature of Ca^{2+} uptake that is coherent with spontaneity and favorable properties as discussed on R_L.

Table 4
Thermodynamic parameters for exchange adsorption of Ca^{2+} by NaCC

ΔH° (kJ/mol)	ΔS° (kJ/(mol·K))	ΔG° (kJ/mol)			R^2
		30°C	50°C	70°C	
68.472	0.286	–18.657	–23.029	–30.094	0.982

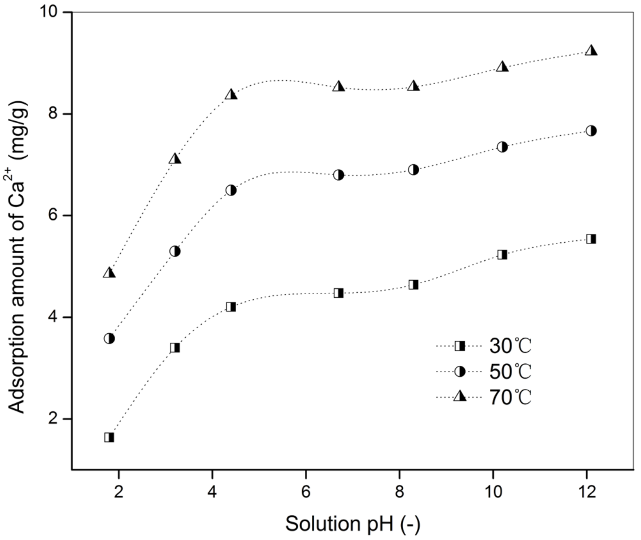

Fig. 8. Effect of pH on adsorption capacity of Ca^{2+} by NaCC under respective solution temperature of 30°C, 50°C and 70°C (initial concentration of Ca^{2+} = 400 mg/L; sampling interval = 3 h).

3.2.3. pH effect

Solution pH is commonly a controlling factor in ion-exchange processes since it may affect the chemistry of adsorbate/adsorbent and in turn the adsorption efficiency. The impact of pH on exchange ability under different temperatures is exhibited in Fig. 8 (pH was adjusted by adding 0.1 M HCl or 0.1 M NaOH solutions). Generally, acid environments presented to be adverse to uptake of Ca^{2+}, which was especially the case when solution pH decreased below 4. This was because under acidic conditions clinoptilolite surface was covered with dissociative hydrogen ions (i.e., H^+) and/or its hydronium form (i.e., H_3O^+), leading to severe competition with Ca^{2+} populations for occupation of the cationic sites on clinoptilolite surface and finally a hindrance of Ca^{2+} adsorption.

For basic condition (pH > 8), elevation of pH somewhat produced an increment on Ca^{2+} adsorption. In fact, clinoptilolite always has a negative surface charge even overwhelmingly surrounded by cationic ions [30], and thus, basic environment with an excessive amount of sodium hydroxide can offer more exchangeable Na^+ sites for Ca^{2+}

adsorption. Meanwhile, the competition of H^+ with Ca^{2+} species substantially got impaired due to limitation of stoichiometry. Then, it is no surprising on the slight enhancement of Ca^{2+} removal under basic pH.

A speciation of $Ca(OH)_2$ should be avoided because it tends to clog the micropores once was generated, with potentiality to lead to an intense reduction of adsorption capacity and lifetime of clinoptilolite. However, there was no formation of calcium hydroxide ($Ca(OH)_2$) within pH range tested (from 1.8 to 12.1), since precipitation of Ca^{2+} with OH^- ligand would take place under pH of at least 12.5 according to the solubility of $Ca(OH)_2$ and concentration of Ca^{2+} (see supplementary material). Result revealed that the tested pH (<12.1) with stoichiometric limitation of H^+ or H_3O^+ will not likely to make considerable ion intervention at solid–liquid interfacial region during adsorption process. This is not the documented case [7] that ascribed decrease of solution alkalinity to conversion of soluble hardness to insoluble products by precipitation on biomaterial substrates (using *Moringa oleifera* seed).

Therefore, we may recommend moderate pH in the range of about 6–8 as the suitable level for application of NaCC, because further rise of pH did not show enough quantitative significance, and more importantly, savings can be made on importation of chemicals for pH adjustment with respect to operational simplicity and cost. Moreover, under whatever pH, it can be seen from Fig. 8 that solution temperature of 70°C always better facilitates Ca^{2+} adsorption than that in lower temperatures.

3.3. Column study

Continuous column systems can minimize the external diffusion limitations by higher driving force for exchange, among which the fixed-bed column [31–34] is basically employed for adsorption/separation purpose in numerous industrial applications. Several operational variables are known to influence the column efficiency including ion concentration of inlet water [33], the flow rate, the sorbent amount as solid phase [34], etc. To extract the information for cooling-water softening, effect of solution temperature on the exchange performance of NaCC was principally investigated in this section.

For column run, the equilibrium adsorption amount of target solute (i.e., aqueous Ca^{2+}) is regarded as an important operational parameter to examine the ability of sorbent, and can be expressed by Eq. (9):

$$q_e = \frac{Q}{1000 \cdot M} \int_0^{t_e} (C_0 - C_e)dt \tag{9}$$

where q_e is the equilibrium amount of Ca^{2+} adsorbed per unit weight of adsorbent, mg/g; Q is the liquid flow rate, mL/min; M is the amount of sorbent in column, g; C_0 and C_e are, respectively, the inlet and effluent concentration of aqueous Ca^{2+}, mg/L; and t_e is the time spent until adsorption equilibrium, min.

Experimental data for q_e are listed in Table 5. It can be seen that elevation of solution temperature from 30°C to 70°C produced a sound enhancement of q_e from 27.87 to 44.64 mg/g, which is not the case for batch experiments where there was little variation of q_e with increasing temperature (about 18.1 mg/g). This is because the ingoing concentration of Ca^{2+} (400 mg/L) for consecutive process can give rise to a maintained external driving force for exchange, whereas for batch experiments the abundance of Ca^{2+} in liquid bulk will accordingly decrease as adsorption process progressed. Thus, mass transfer limitations for batch run overshadowed the intensified affinity of dissociative Ca^{2+} toward surface of clinoptilolite in hot-water environment.

For engineered column reactions, predictive models are commonly utilized for process examination of continuous system serving for process control and scale-up design. Here, the Thomas model [35] was employed as expressed by Eq. (10):

$$\frac{C_e}{C_0} = \frac{1}{1 + \exp[\frac{k_{\mathrm{Th}}}{Q}(q_e M - C_0 V_e)]} \tag{10}$$

where k_{Th} is the Thomas rate constant, mL/(mg·min); V_e is the volume of effluent, mL.

Substitute the term of V_e by Q_t and make a logarithmic conversion of Eq. (10). Then, Eq. (11) can be produced as follows:

$$\ln(\frac{C_0}{C_e} - 1) = \frac{k_{\mathrm{Th}} q_e M}{Q} - \frac{k_{\mathrm{Th}} C_0 t}{1000} \tag{11}$$

By means of linear regression analysis on the term of $\ln(C_0/C_e - 1)$ vs. t, we can obtain the theoretical value of q_e (labeled as q_{et}) from Eq. (11), and relevant parameters obtained by simulation of Thomas model in contrast to experiments are listed in Table 5. Results show that the Thomas model can well predict the equilibrium adsorption amount of Ca^{2+} by NaCC particles with correlation coefficient $R^2 > 0.965$. The Thomas model was developed on the assumption that the adsorption is limited not by chemical interactions but by mass transfer at solid–liquid interface, which is in accordance with the outcome of activation energy (24.71 kJ/mol) assigned to diffusion-limited exchange processes.

Table 5
Parameters of experiments and that obtained by Thomas model on adsorption of Ca^{2+}

Temperature (°C)	M (g)	Z (cm)	C_0 (mg/L)	Q (mL/min)	k_{Th} (mL/(mg·min))	q_{et} (mg/g)	q_e (mg/g)	R^2
30	11.5	20	400	3	0.061	28.37	27.87	0.965
50	11.5	20	400	3	0.084	36.9	36.23	0.966
70	11.5	20	400	3	0.099	44.68	44.64	0.981

The duration of adsorbent is another issue for process evaluation of column work. The breakthrough curves in the presence of NaCC were plotted vs. temperature of 30°C, 50°C and 70°C, respectively, as shown in Fig. 9. It is interesting to note that when solution temperature elevated from 30°C to 70°C, the breakthrough point dramatically got postponed from "a" to "c" point, indicating that an effective uptake of Ca^{2+} by clinoptilolite was prolonged with increasing temperature. The Yoon–Nelson model [36] was introduced to predict the time interval for 50% reduction of solute concentrations as exhibited by Eq. (12):

$$t = \tau + \frac{1}{k_{YN}} \ln \frac{C_e}{C_0 - C_e} \tag{12}$$

where t is the time, min; τ represents time interval for 50% removal of aqueous Ca^{2+}, min; and k_{YN} is the rate constant, min^{-1}.

Linear regression analysis on the term of $\ln C_e/(C_0 - C_e)$ vs. t in Eq. (12) can produce the theoretical value of τ (labeled as τ_t). Relevant parameters are listed in Table 6. Results revealed good suitability of Yoon–Nelson model to simulate the adsorption process for determination of τ with correlation coefficient $R^2 > 0.966$. Analysis data clearly show that τ_t dramatically climbs up from 270.47 to 427.01 min for column run when solution temperature enhanced from 30°C to 70°C. All the results of dynamic adsorption demonstrated that the screening behavior of NaCC packing was substantially strengthened in hydrothermal environment due to the improved exchange capacity and durability. That is to say, NaCC acting as softener should better work in hot waters being typically the case for industrial RCWS.

3.4. Regeneration test

Examination on the reutilization capability of adsorbent is an important step to evaluate the application feasibility and to make the ion-exchange process more economical. For each time of adsorbent regeneration, the spent NaCC underwent the same procedures as introduced for thermal Na^+ conditioning (see section 2.1). The efficiencies of regenerated NaCC sample for removal of Ca^{2+} at different initial concentrations are shown in Fig. 10. For all the cases tested, at least five times replicated use of recovered NaCC can be guaranteed to realize more than 90% removal of Ca^{2+} at initial concentrations lower than 400 mg/L. Reduction of initial Ca^{2+} concentration can globally improve efficiency of replicated utilization of NaCC, among which at least nine times utilization of regenerated NaCC can be ensured for more than 85% removal of aqueous Ca^{2+} once its initial concentration reduced below 40 mg/L. Results showed that NaCC could be repeatedly used for ion exchange of Ca^{2+} with slight loss of initial exchange capacities. Economic figures are presently not available, and there is a need of efforts made for further studies at pilot-scale level in industrial cooling-water systems to provide necessary data for potential filed applications.

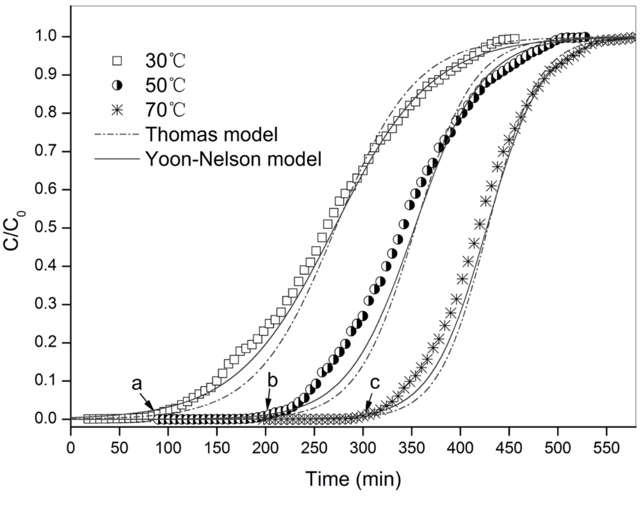

Fig. 9. Breakthrough curves for Ca^{2+} uptake by NaCC under respective temperature of 30°C, 50°C and 70°C (initial concentration of Ca^{2+} = 400 mg/L; amount of NaCC = 11.5 g; flow rate = 3 mL/min).

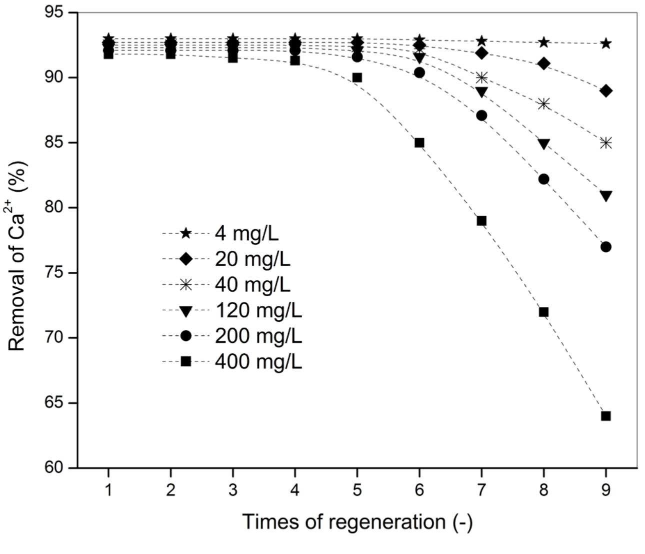

Fig. 10. Times of adsorbent regeneration vs. removal of Ca^{2+} at various initial concentrations (amount of NaCC = 1 g; solution pH = 6.7; temperature = 70°C; sampling interval = 48 h).

Table 6
Relevant parameters of Yoon–Nelson model on adsorption of aqueous Ca^{2+}

Temperature (°C)	M (g)	Z (cm)	C_0 (mg/L)	Q (mL/min)	k_{YN} (min^{-1})	τ_t (min)	τ (min)	R^2
30	11.5	20	400	3	0.025	270.47	264	0.966
50	11.5	20	400	3	0.034	352.88	348	0.970
70	11.5	20	400	3	0.040	427.01	426	0.983

4. Conclusions

Clinoptilolite is abundant on earth owning merits of hydrothermal/mechanical stability and surface modifiability. Chemical conditioning by exchangeable cation (such as Na^+) could enable clinoptilolite working as softener for RCWS. In this work, NC was thermally conditioned by NaCl solution as functionalized adsorbent (namely NaCC) dealing with Ca^{2+} as typical hardness ion. To extract application possibility, preliminary experiments in both batch and column modes were carried out, and the performances of NaCC were evaluated under different temperature environments (respective 30°C, 50°C, and 70°C).

Results demonstrated that Na^+ conditioning of clinoptilolite largely enhanced exchangeability toward aqueous Ca^{2+} (three-time conditioning allowed optimal Ca^{2+} abatement). Elevation of solution temperature clearly accelerated the uptake of Ca^{2+} for all the cases tested, and equilibrium adsorption capacity for continuous run got improved in hotter environment due to a stable external driving force for exchange. Predictive models are successfully used to evaluate temperature effect on: (1) the fundamental parameters of kinetics, isotherms and thermodynamics (for batch study) that provide insights into the adsorption pathways, adsorbent affinity, etc., and (2) the breakthrough curves (for column tests) that leave the information of equilibrium adsorption capacity, durability of solid packing, etc. Moreover, experiments suggested that moderate solution pH is suitable enough for functionalization of NaCC (need not further adjustment), and regeneration studies revealed that at least five cycles replicated utilization can be allowed for more than 90% removal of Ca^{2+} at concentrations within 400 mg/L. As a consequence, NaCC may be further recommended as effective softener serving for industrial RCWS cases.

Acknowledgments

The authors gratefully acknowledge financial support by National Natural Science Foundation of China (No. 51608349), Natural Science Foundation of Tianjin (15JCYBJC49100), and Open Foundation of Key Laboratory of Industrial Ecology and Environmental Engineering (1500-842001).

References

[1] S. Ashwini, Fouling control of PVC film-type cooling tower fills at power plants, Mater. Perform., 47 (2008) 50–54.

[2] B.A. Qureshi, S.M. Zubair, A complete model of wet cooling towers with fouling in fills, Appl. Therm. Eng., 26 (2006) 1982–1989.

[3] J. Sheng, H. Zhang, Precipitation characteristics of $CaCO_3$ scaling on stainless steel in cooling tower condition, Appl. Mech. Mater., 226–228 (2012) 1029–1033.

[4] F.P. Yu, L.D. Ginn, W.F. McCoy, Cooling tower fill fouling control in a geothermal power plant, Corros. Rev., 17 (1999) 205–217.

[5] F. Jones, P. Jones, M.I. Ogden, W.R. Richmond, A.L. Rohl, M. Saunders, The interaction of EDTA with barium sulfate, J. Colloid Interface Sci., 316 (2007) 553–561.

[6] G.J. Millar, S. Papworth, S.J. Couperthwaite, Exploration of the fundamental equilibrium behaviour of calcium exchange with weak acid cation resins, Desalination, 351 (2014) 27–36.

[7] S.A. Muyibi, L.M. Evison, *Moringa oleifera* seeds for softening hardwater, Water Res., 29 (1995) 1099–1104.

[8] M.R. Awual, A. Jyo, Assessing of phosphorus removal by polymeric anion exchangers, Desalination, 281 (2011) 111–117.

[9] W. Mozgawa, M. Krol, W. Pichor, Use of clinoptilolite for the immobilization of heavy metal ions and preparation of autoclaved building composites, J. Hazard. Mater., 168 (2009) 1482–1489.

[10] C. Wang, Y. Li, H.S. Shi, J.F. Huang, Preparation and characterization of natural zeolite supported nano TiO_2 photocatalysts by a modified electrostatic self-assembly method, Surf. Interface Anal., 47 (2015) 142–147.

[11] V.J. Inglezakis, M.M. Loizidou, H.P. Grigoropoulou, Ion exchange studies on natural and modified zeolites and the concept of exchange site accessibility, J. Colloid Interface Sci., 275 (2004) 570–576.

[12] M.V. Mier, R.L. Callejas, R. Gehr, B.E.J. Cisneros, P.J.J. Alvarez, Heavy metal removal with Mexican clinoptilolite: multi-component ionic exchange, Water Res., 35 (2001) 373–378.

[13] L. Mihaly-Cozmuta, A. Mihaly-Cozmuta, A. Peter, C. Nicula, H. Tutu, D. Silipas, E. Indrea, Adsorption of heavy metal cations by Na-clinoptilolite: equilibrium and selectivity studies, J. Environ. Manage., 137 (2014) 69–80.

[14] N. Rajic, D. Stojakovic, M. Jovanovic, N.Z. Logar, M. Mazaj, V. Kaucic, Removal of nickel(II) ions from aqueous solutions using the natural clinoptilolite and preparation of nano-NiO on the exhausted clinoptilolite, Appl. Surf. Sci., 257 (2010) 1524–1532.

[15] S.A. Abdulkareem, E. Muzenda, A.S. Afolabi, J. Kabuba, Treatment of clinoptilolite as an adsorbent for the removal of copper ion from synthetic wastewater solution, Arab. J. Sci. Eng., 38 (2013) 2263–2272.

[16] E. Chmielewska, L. Sabova, H. Peterlik, A. Wu, Batch-wise adsorption, saxs and microscopic studies of zeolite pelletized with biopolymeric alginate, Braz. J. Chem. Eng., 28 (2011) 63–71.

[17] M.K. Doula, Removal of Mn^{2+} ions from drinking water by using clinoptilolite and a clinoptilolite-Fe oxide system, Water Res., 40 (2006) 3167–3176.

[18] Y. Zhao, Y.C. Niu, X. Hu, B.D. Xi, X. Peng, W.F. Liu, W.X. Guan, L. Wang, Removal of ammonium ions from aqueous solutions using zeolite synthesized from red mud, Desal. Wat. Treat., 57 (2016) 4720–4731.

[19] M. Rozic, S. Cerjan-Stefanovic, S. Kurajica, M.R. Maeefat, K. Margeta, A. Farkas, Decationization and dealumination of clinoptilolite tuff and ammonium exchange on acid-modified tuff, J. Colloid Interface Sci., 284 (2005) 48–56.

[20] L.L. Ames, The cation sieve properties of clinoptilolite, Am. Mineral., 45 (1960) 689–700.

[21] Y.F. Wang, F. Lin, Synthesis of high capacity cation exchangers from a low-grade Chinese natural zeolite, J. Hazard. Mater., 166 (2009) 1014–1019.

[22] A.H. Ören, A. Kaya, Factors affecting adsorption characteristics of Zn^{2+} on two natural zeolites, J. Hazard. Mater., 131 (2006) 59–65.

[23] D. Mohan, K.P. Singh, Single- and multi-component adsorption of cadmium and zinc using activated carbon derived from bagasse—an agricultural waste, Water Res., 36 (2002) 2304–2318.

[24] Y.S. Huo, T.H. Chiang, Y.M. Hsueh, Removal of basic dye from aqueous solution using tree fern as a biosorbent, Process Biochem., 40 (2005) 119–124.

[25] M.J. Zamzow, B.R. Eichbaum, K.R. Sandgren, D.E. Shanks, Removal of heavy metals and other cations from wastewater using zeolites, Sep. Sci. Technol., 25 (1990) 1555–1569.

[26] S. Kesraouiouki, C. Cheeseman, R. Perry, Effects of conditioning and treatment of chabazite and clinoptilolite prior to lead and cadmium removal, Environ. Sci. Technol., 27 (1993) 1108–1116.

[27] H. Nollet, M. Roels, P. Lutgen, P. Van der Meeren, W. Verstraete, Removal of PCBs from wastewater using fly ash, Chemosphere, 53 (2003) 655–665.

[28] Y.S. Ho, J.C.Y. Ng, G. McKay, Kinetics of pollutant sorption by biosorbents: review, Sep. Purif. Methods, 29 (2000) 189–232.

[29] A.M. Donia, A.A. Atia, H.A. El-Boraey, D.H. Mabrouk, Adsorption of Ag(I) on glycidyl methacrylate/*N*,*N*′-methylene bis-acrylamide chelating resins with embedded iron oxide, Sep. Purif. Technol., 48 (2006) 281–287.

[30] S. Çoruh, O.N. Ergun, Ni^{2+} removal from aqueous solutions using conditioned clinoptilolites: kinetic and isotherm studies, Environ. Prog. Sustain. Energy, 28 (2009) 162–172.

[31] A.H. Nguyen, H.H. Ngo, W.S. Guo, T.Q. Pham, F.M. Li, T.V. Nguyen, X.T. Bui, Adsorption of phosphate from aqueous solutions and sewage using zirconium loaded okara (ZLO): fixed-bed column study, Sci. Total Environ., 523 (2015) 40–49.

[32] M.A. Fulazzaky, M.H. Khamidun, M.F.M. Din, A.R.M. Yusoff, Adsorption of phosphate from domestic wastewater treatment plant effluent onto the laterites in a hydrodynamic column, Chem. Eng. J., 258 (2014) 10–17.

[33] V. Vivacqua, W.J. Xu, G. Hébrard, L.Y. Li, J.R. Grace, Modeling of zinc adsorption onto clinoptilolite in a slurry bubble column, Chem. Eng. Sci., 100 (2013) 326–331.

[34] T.C. Nguyen, P. Loganathan, T.V. Nguyen, S. Vigneswaran, J. Kandasamy, R. Naidu, Simultaneous adsorption of Cd, Cr, Cu, Pb, and Zn by an iron-coated Australian zeolite in batch and fixed-bed column studies, Chem. Eng. J., 270 (2015) 393–404.

[35] H. Paudyal, B. Pangeni, K. Inoue, H. Kawakita, K. Ohto, S. Alam, Adsorptive removal of fluoride from aqueous medium using a fixed bed column packed with Zr(IV) loaded dried orange juice residue, Bioresour. Technol., 146 (2013) 713–720.

[36] R. Sharma, B. Singh, Removal of Ni(II) ions from aqueous solutions using modified rice straw in a fixed bed column, Bioresour. Technol., 146 (2013) 519–524.

Supplementary data

1. Discussion on speciation of $Ca(OH)_2$

In response to increment of solution pH, the speciation of $Ca(OH)_2$ may take place affecting process analysis as well as material evaluation, and this possibility should be avoided because $Ca(OH)_2$ tends to clog the micropores of zeolite that can lead to an intense reduction of adsorption capacity and lifetime. Read S-Table 1, precipitation of Ca^{2+} with OH^- ligand would take place under pH of at least 12.5 according to the solubility of $Ca(OH)_2$ and concentration of Ca^{2+}. This result indicates that there was almost no formation of $Ca(OH)_2$ within the tested pH range (from 1.8 to 12.1 in this work).

2. Dosage effect of NaCC (batch study)

In theory, the more Ca^{2+} species as hardness ion presents in solution sample, the higher dosage of material should be required to achieve an equivalent adsorptive removal target. And this is indeed the case since removal rate of Ca^{2+} was found to increase with increasing dosage of NaCC as recorded in S-Table 2. Within a same time interval meanwhile, the uptake of Ca^{2+} for each unit mass of adsorbent exhibited to decrease, which is opposite to the trend of total Ca^{2+} removal. We can also see from S-Table 2 that the simulated hydrothermal environment of cooling water (70°C) favors better performance of NaCC in both the efficiency and capacity of ion exchange.

3. Impact of operational variables on column tests

The fixed-bed column is basically employed for adsorption/separation purpose in numerous industrial applications. Data of temperature effect has been presented and discussed in the main text of manuscript (see section 3.3 in text). As supplementary material, effects of other operational variables including the flow rate, inlet concentration of Ca^{2+} and the packing height are listed in S-Table 3, for which solution temperature of 30°C was selected as an example of case study.

S-Table 1
Parameters for solubility of $Ca(OH)_2$ and precipitation of aqueous Ca^{2+}

Temperature (°C)	Solubility (g/100 g H_2O)	K_{sp}[a]	Ca^{2+} concentration (mol/L)	$[OH]^{-b}$ (mol/L)	pH_{pre}[c]
30	0.153	3.54×10^{-5}	0.01	0.059	12.8
50	0.138	2.59×10^{-5}	0.01	0.051	12.7
70	0.106	1.18×10^{-5}	0.01	0.034	12.5

[a] K_{sp} was determined by $s = (K_{sp}/4)^{1/3}$ since $Ca(OH)_2$ molecule belongs to AB_2 type.

[b] Critical concentration of OH^- was determined by $K_{sp} = [Ca^{2+}]\cdot[OH^-]^2$ on formation of $Ca(OH)_2$.

[c] pH_{pre} denotes the least pH value for the formation of $Ca(OH)_2$.

S-Table 2
Dosage effect of NaCC on the uptake of aqueous Ca^{2+} (initial Ca^{2+} concentration = 400 mg/L, sampling time = 3 h)

NaCC amount (g)	Capacity (mg/g)			Rate (%)		
	30°C	50°C	70°C	30°C	50°C	70°C
0.5	5.24	9.43	13.20	13.23	23.77	33.27
1.0	4.67	8.10	11.04	23.20	40.75	55.19
1.5	3.95	6.59	9.00	29.59	49.17	69.15
2.0	3.53	5.64	7.48	35.23	56.02	74.29

S-Table 3
Adsorption of Ca^{2+} by NaCC with different operational variables

Q (mL/min)	Z (cm)	C_0 (mg/L)	q_{max} (mg/g)	q_e (mg/g)	Rate (%)
1.5	20	400	328.76	29.40	64.34
2	20	400	320.06	28.48	64.22
3	20	400	319.28	27.87	63.49
3.5	20	400	307.30	25.78	61.86
4	20	400	275.52	23.75	60.87
3	20	200	302.94	26.44	63.91
3	20	400	319.28	27.87	63.49
3	20	600	324.77	28.35	62.30
3	5	400	37.42	13.20	58.33
3	10	400	117.61	20.36	61.11
3	15	400	176.42	20.81	61.88
3	18	400	256.61	24.18	62.34
3	20	400	319.28	27.87	63.49